Dynamics of Bacterial and Viral Transmission in Experimental Microbiota Transplantation

James S. Weagley[1], Luis Alberto Chica Cárdenas[1], Ana Romani[1], Meagan E. Sullender[1], Somya Aggarwal[1], Heyde Makimaa[1], Michael P. Hogarty[1], Rachel Rodgers[1,2], Elizabeth A. Kennedy[1], Lynne Foster[1], Lawrence A. Schriefer[1], Megan T. Baldridge[1,3#]

[1] Division of Infectious Diseases, Department of Medicine, Edison Family Center for Genome Sciences & Systems Biology, Washington University School of Medicine, St. Louis, MO, USA

[2] Department of Pediatrics, Washington University School of Medicine, St. Louis, MO, USA.

[3] Department of Molecular Microbiology, Washington University School of Medicine, St. Louis, MO, USA.

[#] Correspondence: mbaldridge@wustl.edu

Abstract

Mouse models are vital tools for discerning the relative contributions of host and microbial genetics to disease, often requiring the transplantation of microbiota between different mouse strains. Transfer methods include antibiotic treatment of recipients and colonization using either co-housing with donors or the transplantation of fecal or cecal donor material. However, the efficiency and dynamics of these methods in reconstituting recipients with donor microbes is not well understood. We thus directly compared co-housing, fecal transplantation, and cecal transplantation methods. Donor mice from Taconic Biosciences, possessing distinct microbial communities, served as the microbial source for recipient mice from Jackson Laboratories, which were treated with antibiotics to disrupt their native microbiota. We monitored bacterial and viral populations longitudinally over the course of antibiotics treatment and reconstitution using 16S rRNA gene sequencing, quantitative PCR, and shotgun sequencing of viral-like particles. As expected, antibiotic treatment rapidly depleted microbial biomass and diversity, with slow and incomplete natural recovery of the microbiota in non-transplanted control mice. While all transfer methods reconstituted recipient mice with donor microbiota, co-housing achieved this more rapidly for both bacterial and viral communities. This study provides valuable insights into microbial transfer methods, enhancing reproducibility and informing best practices for microbiota transplantation in mouse models.

Introduction

As appreciation grows for the diverse range of phenotypes the microbiota can mediate so does our reliance on manipulatable small animal models to experimentally interrogate these effects. The gut microbiota, a complex community of microorganisms residing in the gastrointestinal tract, plays a pivotal role in host health and physiology[1,2]. These microbial communities are involved in critical functions such as nutrient metabolism[3,4], immune system development[5–7], and protection against pathogens[8–10]. Dysbiosis, or the disruption of the normal microbiota balance, has been implicated in a range of diseases including obesity[11,12], malnutrition[13,14], and inflammatory bowel diseases[15,16]. Understanding the intricate relationships between the microbiota and host systems is therefore essential for developing therapeutic strategies targeting microbiota-related diseases.

To unravel these complex host-microbe interactions, researchers heavily leverage animal models, particularly mice. Controlled studies using mouse models enable the manipulation of microbial communities to observe resultant effects on host physiology and disease outcomes. A key aspect of such research is the generation of gnotobiotic mice—animals that are germ-free or colonized with specific, defined microbial communities[17]. These models provide a unique platform to study the microbiota's role under controlled conditions. Despite the utility of germ-free mice for numerous applications, however, their use is associated with some drawbacks. For investigators studying numerous mouse genotypes, executing experiments not amenable to the use of a gnotobiotic isolator such as those involving particular pathogens or behavioral testing, or performing studies requiring a normal microbiota during development which is then disrupted, germ-free mice may be impractical or inappropriate. Antibiotics treatment represents an cost-effective and accessible alternative for the depletion of the microbiota, and this approach has been broadly used by many investigators to examine many of the same phenotypes explored in germ-free mice, often with strong concordance between the two models[17].

Establishing gnotobiotic mice or reconstituting the microbiota after perturbation necessitates reliable and efficient methods for microbial transfer. Common techniques include

65 fecal microbiota transplantation, cecal content transplantation, and co-housing. Fecal
66 transplantation involves transferring fecal material from a donor to a recipient via the oral route,
67 while cecal transplantation is similar but utilizes the cecal contents, which may have a different
68 microbiota. Co-housing leverages the natural coprophagic behavior of mice to transfer
69 microbes. Despite their widespread use, experiments designed utilizing these methods are
70 generally based on historical precedent rather than a comprehensive understanding of their
71 efficacy or the specific dynamics of microbial colonization they promote.

72 This reliance on convention can lead to assumptions that impact experimental
73 outcomes and reproducibility, a major challenge facing the field[18–21]. For instance, variation in
74 microbial transfer efficiency can affect the establishment of the desired microbiota, influencing
75 the host's physiological responses and potentially skewing results[22,23]. Furthermore, while
76 bacterial community dynamics have been relatively well-studied, the transfer and
77 establishment of viral communities (the virome) remain less understood. Given the growing
78 recognition that bacteriophages and other viruses shape microbial communities and influence
79 host health[24–30], it is crucial to consider both bacterial and viral components when evaluating
80 these methods. A comprehensive virome analysis is essential.

81 Herein, we systematically compare fecal transplantation, cecal transplantation, and co-
82 housing as methods for transferring microbes to microbially depleted mice, characterizing this
83 process longitudinally. Recipient mice from Jackson Laboratories were treated with antibiotics
84 for one week to disrupt their native microbiota. Donor mice from Taconic Biosciences, known
85 to have distinct microbial communities from Jackson, served as the source of bacteria and
86 viruses for transplantation[31]. By employing 16S rRNA gene sequencing and quantitative PCR
87 (qPCR), we monitored bacterial load, diversity, and composition. Additionally, we analyzed
88 viral community composition and diversity through short-read shotgun sequencing of viral-like
89 particles. We employed a comprehensive contig-based, annotation-agnostic strategy in
90 conjunction with in-depth classification and binning of viral-like particle (VLP) sequences,
91 allowing for an unbiased characterization of both known and novel viruses. Thus, we provide

a more complete landscape of virome dynamics than would be possible with annotation-dependent methods alone.

We find that co-housing facilitates a more rapid transfer of both bacterial and viral communities compared to fecal and cecal transplants, which performed similarly to each other. Viral communities generally tracked with bacterial colonization, though each method enriched for distinct bacterial taxa—and their associated phages—at different timepoints. These results highlight method-specific influences on microbial community dynamics and underscore the importance of method selection in experimental design.

By carefully characterizing these commonly used methods, our study provides valuable insights that can enhance reproducibility and consistency in microbiota research. This work informs best practices for replacing the enteric microbiota of mice and contributes to our understanding of the mechanisms underlying microbial transfer and establishment in experimental models. Such insights are essential for advancing microbiota research and for the development of interventions targeting microbiota-related diseases.

107 **Results**

108 *Effect of antibiotic treatment on bacterial load, diversity, and community composition*

109 To evaluate the impact of antibiotic treatment on bacterial load, diversity, and
110 community composition, we treated C57BL/6 mice from Jackson Laboratory (JAX) with a
111 simplified antibiotic cocktail of vancomycin, neomycin, and ampicillin for seven days. This
112 regimen, shown by us and others to mediate robust depletion of the microbiota within three to
113 seven days while being well-tolerated by recipients[10,11], was administered to JAX recipient
114 mice. C57BL/6 mice from Taconic (TAC), which are well-established to harbor distinct enteric
115 microbial communities compared to JAX mice[12,13], served as microbiota donors, while
116 untreated JAX and TAC mice served as controls (**Extended Data Fig. 1A**). Fecal samples
117 were collected on days 0, 1, 3, and 7 for 16S rRNA gene qPCR and sequencing. At baseline
118 (day 0), bacterial load was not significantly different between JAX and TAC mice (**Extended**
119 **Data Fig. 1B**, $p > 0.05$). By day 1, antibiotics significantly reduced bacterial load in JAX mice
120 ($p < 0.05$), with 16S levels falling below the limit of detection by day 7 (**Extended Data Fig.**
121 **1B**). Bacterial load remained stable in untreated controls.

122 Sequencing of the V4 region of the 16S rRNA gene was performed and analyzed using
123 the DADA2 pipeline implemented in Nephele to generate amplicon sequence variants (ASVs),
124 which were grouped into bacterial species based on >97% sequence identity[32,33]. Initial ASV
125 richness was comparable between JAX and TAC mice (mean ± SE: TAC = ~80 ± 6 OTUs,
126 JAX = 66 ± 5; **Extended Data Fig. 1C**). Antibiotic treatment significantly reduced species
127 richness within one day compared to Jackson controls (mean ± SE: 43 ± 6 and 117 ± 2.4,
128 respectively), with richness dropping to approximately one-sixth of the original level by day 7
129 (**Extended Data Fig. 1C**, 9.3 ± 0.9), although sequencing suggested some native bacteria
130 persisted at low levels. To assess changes in community composition, unweighted UniFrac
131 distances were calculated and visualized using principal coordinate analysis (PCoA). PCoA
132 axis 1 explained 24.6% of the total variance, primarily reflecting antibiotic-induced shifts in
133 JAX mice, while axis 2 (13.0%) separated untreated JAX and TAC samples (**Extended Data**
134 **Fig. 1D**). Antibiotic treatment had a greater impact on microbial community composition than

135 mouse vendor. These results demonstrate that one week of vancomycin, neomycin, and
136 ampicillin treatment is sufficient to drastically reduce bacterial load and diversity and
137 significantly alter gut microbiota composition.
138
139

140 *Route of transfer regulates community reconfiguration during transplantation following*
141 *antibiotic treatment*

142 We compared the outcomes of different transfer methods for transplanting TAC
143 microbiota into antibiotic-treated JAX mice. Antibiotics were stopped on day 7, and mice were
144 either maintained without intentional microbial transfer, gavaged on day 8 and 9 with prepared
145 cecal material or fecal material or co-housed with untreated TAC donors for two weeks (**Fig.**
146 **1A**). TAC and JAX mice that didn't receive antibiotics were also monitored over the same
147 period.

148 Bacterial load increased significantly by day 9 in all transplanted mice, regardless of
149 method, compared to non-transplanted mice (**Fig. 1B**). While non-transplanted mice also
150 showed detectable bacterial levels by day 9, their loads were nearly two orders of magnitude
151 lower than those of transplanted or untreated control mice. By day 11, 16S copy numbers
152 were comparable across all groups, and by day 14, bacterial loads remained similar for the
153 rest of the experiment. In contrast, recovery of bacterial alpha-diversity progressed more
154 slowly than bacterial load, particularly for the gavage based transplantation methods (**Fig. 1C**)

155 The effect of the transplant method on community composition was evaluated.
156 Samples were separated by collection day and treatment group. Unweighted UniFrac
157 distances assessed global changes in community composition and beta diversity. PCoA
158 visualized microbial community recovery and transfer between days 7 and 21 (**Fig. 1D**).
159 Confidence ellipses represented the original recipient (JAX) and donor (TAC) communities in
160 feces from untreated mice from days 0 through 7.

161 Bacterial communities of antibiotic-treated JAX mice administered fecal or cecal
162 transplants gradually approached the TAC donor community composition between days 9 and
163 11, converging by day 15 (**Fig. 1D**). While fecal or cecal transplant restored bacterial loads to
164 TAC donor levels within two days (**Fig. 1B**), the community composition wasn't fully
165 recapitulated by day 9. In contrast, co-housed mice exhibited bacterial compositions
166 equivalent to TAC donors after only two days (**Fig. 1D, E**). JAX mice that received antibiotics,

167 but no transfer gradually returned towards untreated JAX mice, achieving a similar state to the
168 original microbiota by day 21.

169 The unweighted UniFrac distances of treatment arms compared to untreated Taconic
170 and Jackson control mice were analyzed using PERMANOVA. To account for temporal
171 community composition drift and low sample sizes in untreated Taconic controls, daily
172 treatment arm samples were compared to pooled control samples within the same week.
173 Antibiotic-treated animals differed significantly from JAX controls after 1 day, with this
174 difference persisting until day 7 (**Fig. 1E**). The bacterial community of all groups differed from
175 TAC controls, increasing until day 7 (**Figs. 1D, E**). By day 9, antibiotic-treated JAX mice co-
176 housed with TAC donors were no longer significantly different from TAC controls. Cecal or
177 fecal transfer recipients differed from Taconic donors until day 14, suggesting varying transfer
178 efficiency. Consistent with their bacterial loads (**Fig. 1B**), antibiotic-treated JAX mice
179 recovered and were not significantly different from JAX controls by day 21 (**Figs. 1D, E**).
180 However, the average distance between these groups remained elevated (mean ± SD: 0.69
181 ± 0.1) and hadn't returned to baseline (mean ± SD: 0.47 ± 0.1). Co-housed mice showed the
182 fastest transition to a TAC-like community but weren't significantly different from JAX controls
183 on days 14 and 21, though different on day 15. This may indicate incomplete microbial transfer
184 or JAX bacteria recovery in co-housed mice, resulting in an 'intermediate' community state.

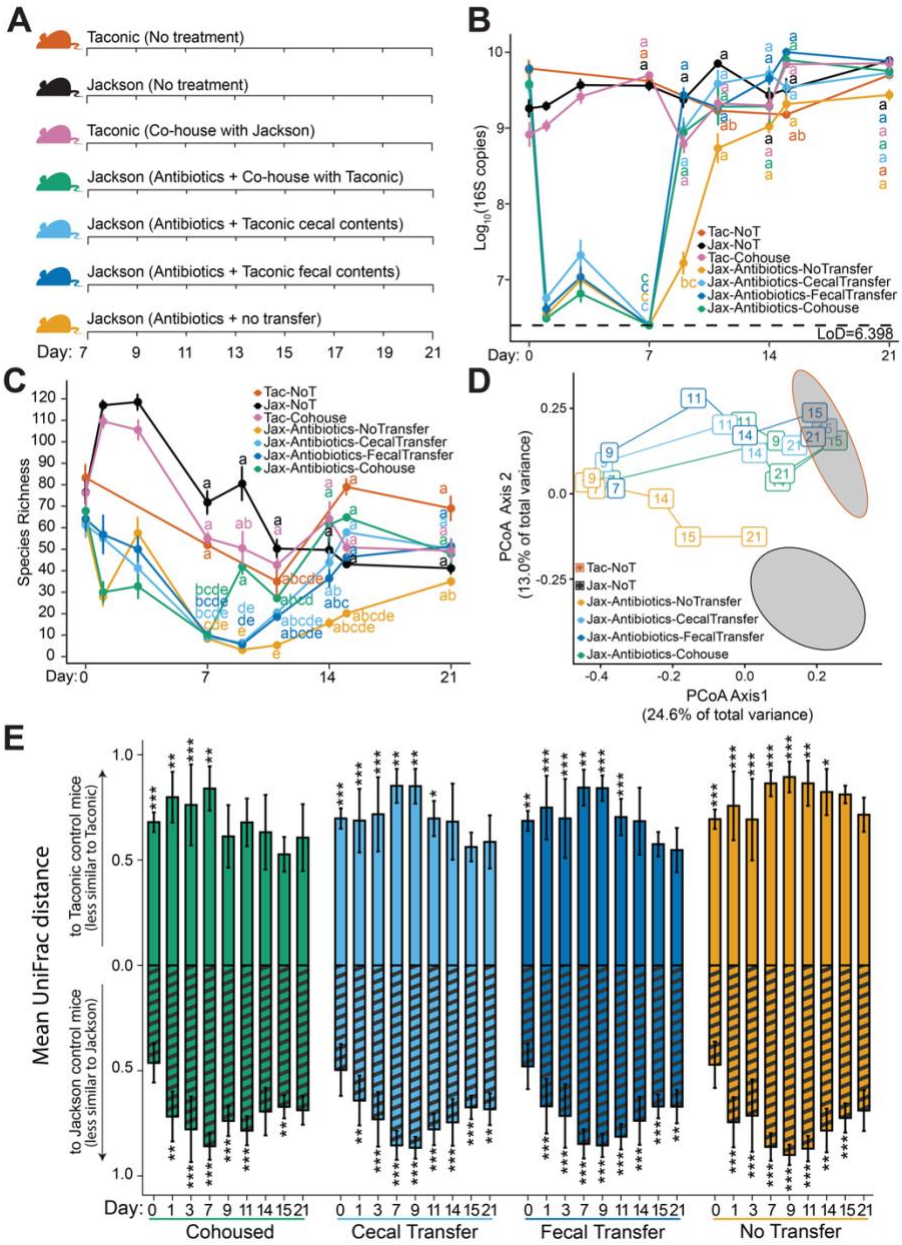

Figure 1. Cohousing of mice reconstitutes the bacterial microbiota more rapidly than fecal or cecal transplant. (**A**) Antibiotic-treated Jackson mice were either allowed to recover naturally (Jax-Antibiotics-NoTransfer; n=12, 8-12 samples per timepoint across three experiments), or were colonized with Taconic-associated microbes via gavage of cecal (Jax-Antibiotics-CecalTransfer; n=12, 7-12 samples per timepoint) or fecal (Jax-Antibiotics-FecalTransfer; n=12, 8-12 samples per timepoint) material, or co-housing (Jax-Antibiotics-Cohouse; n=11, 6-11 samples per timepoint). Jackson (Jax-NoT) and Taconic (Tac-NoT) mice that did not receive antibiotics were maintained as controls. (**B**) Bacterial load measured by qPCR of the 16S rRNA gene throughout the final two weeks of the experiment shows the rapid recovery of bacterial load following transplantation. The letters next to each point indicate significant groupings, those with the same letter were not significantly different from one another by two-way ANOVA followed by Tukey's HSD post-hoc test for pairwise comparisons with an alpha of 0.05 (**C**) Bacterial species richness, the number of unique bacterial species observed per mouse, throughout the first week of the experiment via v4-16s sequencing. The letters next to each point indicate significant groupings, those with the same letter were not significantly different from one by Kruskal-Wallis followed by Bonferroni's correction for multiple comparisons with an alpha threshold of 0.05. (**D**) Principal Coordinate Analysis of

203 unweighted UniFrac distances calculated from species counts across all three weeks of the
204 experiment illustrate the change in community composition following antibiotic treatment and
205 microbiota transplantation. Ellipses (95% confidence) represent the baseline fecal bacterial
206 communities of untreated Jackson (Jax-NoT) and Taconic (Tac-NoT) mice during the first
207 week of the experiment. (**E**) Bar heights indicate the mean Unweighted UniFrac distance was
208 calculated between the fecal bacterial community of Jackson mice treated with antibiotics that
209 received microbial transplantation via co-housing, cecal transfer, fecal transfer, or no transfer,
210 and the fecal bacterial community of control Jackson and Taconic mice that never received
211 antibiotics, pooled by week (days pooled: [0,7), [7,14), [14,21]). Striped bars below the x-axis
212 indicate the distance from untreated Jackson controls while solid bars above the x-axis
213 indicate the distance from untreated Taconic controls. Error bars indicate the standard
214 deviation of all pairwise comparisons between the indicated groups. A PERMANOVA test was
215 performed on the unweighted UniFrac distance matrix for the comparisons shown followed by
216 Bonferroni's corrections for multiple comparisons (* $p < 0.05$, ** $p < 0.01$, *** $p < 0.001$).
217
218

219 *Co-housing rapidly transfers Taconic-associated bacterial taxa and their predicted functional*
220 *capabilities*

221 To understand bacterial transfer following transplantation, ASVs were classified as
222 TAC- (162 ASVs), JAX-associated (124 ASVs), or neither/both based on their prevalence in
223 untreated mice in the samples collected during the first week of the experiment (50 TAC and
224 81 JAX samples) (**Fig. 2A**). These subsets were tracked throughout the experiment. TAC
225 ASVs were higher in TAC mice than in untreated JAX mice, significantly so on days 7 and 8.
226 Although there was a transient increase in the richness of TAC ASVs on days 1 and 3 in all
227 groups measured, by day 7 the TAC-associated ASV richness in all JAX mice (mean = 0.7 –
228 2.6 Taconic ASVs per sample) was significantly lower than in TAC donors (~36.3 Taconic
229 ASVs per sample) (**Fig. 2B**). By day 9, TAC ASVs increased in co-housed mice (mean ± SE
230 = 26.9 ± 2.0) and were higher than untreated JAX controls (mean ± SE = 0.7 ± 0.1) but not
231 significantly different from TAC co-housed donors (mean ± SE = 30.8 ± 4.5). At day 9, cecal
232 or fecal transplants didn't significantly increase TAC-associated ASV richness (means ± SEs
233 = 4.6 ± 0.8 and 4.3 ± 0.4, respectively). By day 15, the richness of TAC-associated ASVs in
234 JAX mice that received antibiotics followed by cecal or fecal transplant was significantly
235 elevated relative to Jackson control mice and remained relatively steady until the end of the
236 experiment on day 21. Co-housing introduced donor-specific bacteria more rapidly than cecal
237 or fecal transplant.

238 To characterize the functional capacity of bacterial communities, we used PICRUSt2
239 to predict the abundance of MetaCyc pathways in each sample[34,35]. We compared antibiotic-
240 treated JAX mice and TAC co-housed donors to JAX and TAC controls grouped by week to
241 identify differentially abundant pathways using DESeq2 (**Fig. 2C**)[36]. A larger number of
242 differentially abundant pathways indicates greater functional disparity. Consistent with our
243 taxonomic results, the number of differentially abundant pathways between co-housed JAX
244 mice and TAC control mice dropped off rapidly, from over 200 on day 7 to less than 100 on
245 day 9. Mice receiving a cecal transplant didn't drop below 100 until day 14, while fecal
246 transplant recipients didn't until day 21. Co-housing led to a more rapid and comprehensive
247 transfer of Taconic-associated bacterial taxa and their predicted functional capabilities
248 compared to cecal or fecal transplantation.

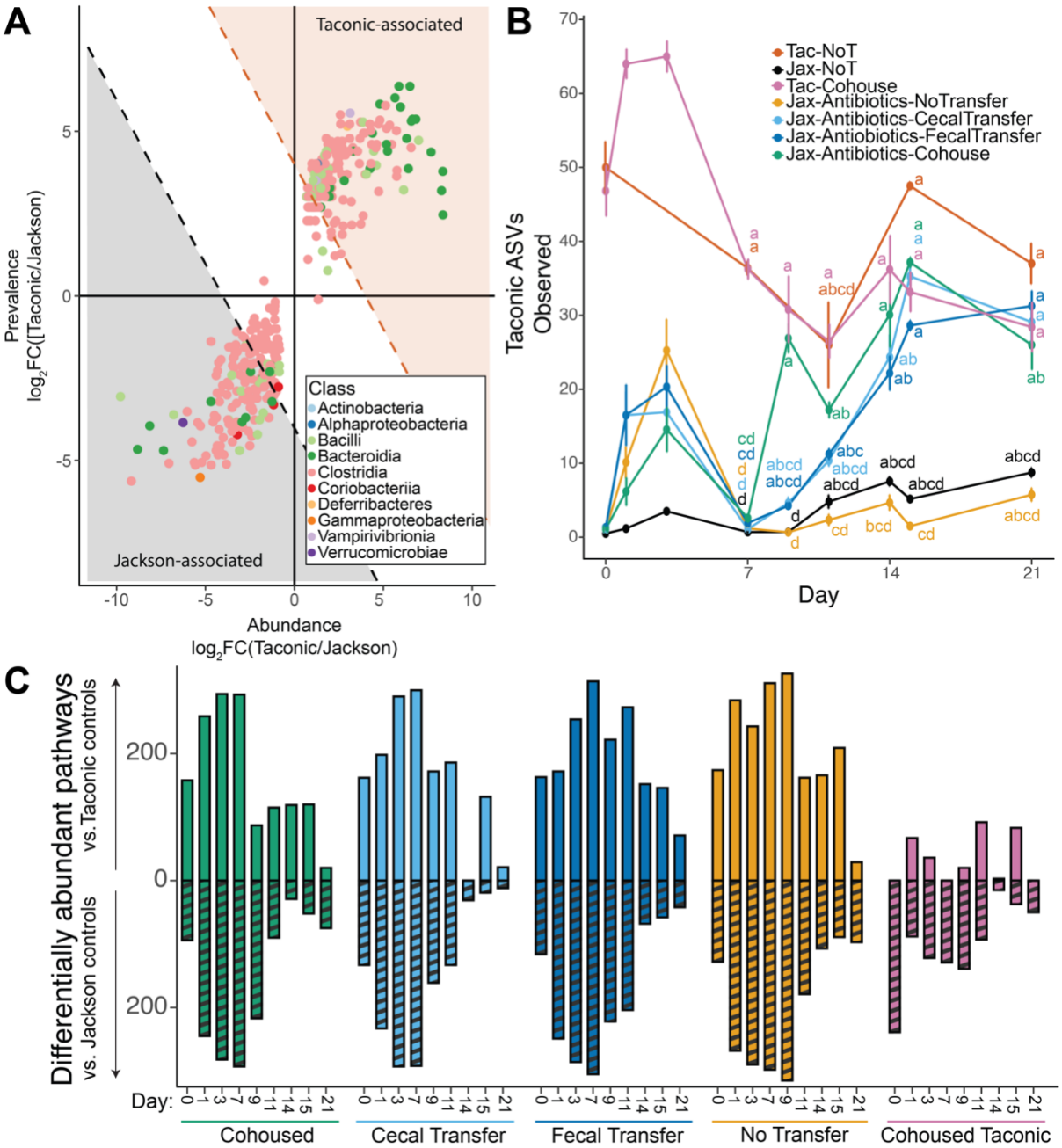

Figure 2. Defining and tracking Taconic-associated ASVs and their predicted functional capacities. (**A**) Bacterial ASVs were defined as being Taconic or Jackson associated based on their prevalence and abundance in samples collected from antibiotics-free JAX (n = 81) and TAC (n=50) mice over the first week of the experiment. ASVs that had an absolute combined $\log_2$(Fold Change) greater than 4 were consider Taconic-associated while those that had an absolute combined $\log_2$(Fold Change) less than -4 were considered Jackson-associated. (**B**) Richness of Taconic ASVs was monitored throughout the course of the experiment, plot show mean richness in each group at a given timepoint, error bars represent the standard error, compact letter display indicates results of pairwise Kruskal-Wallis followed by Bonferroni's correction for multiple comparisons with an alpha threshold of 0.05. (**C**) Abundance of functional pathways were predicted using PICRUSt2. Bar heights indicate the number of pathways determined to be significantly differentially abundant using DESeq2 (alpha = 0.05) to compare between the fecal bacterial community of Jackson mice treated with antibiotics that received microbial transplantation via co-housing, cecal transfer, fecal transfer, or no transfer, and Taconic co-housed mice, and the fecal bacterial community of control

Jackson and Taconic mice that never received antibiotics, pooled by week (days pooled: [0,7), [7,14), [14,21]).

269 *Transfer of specific bacterial taxa differs between methods of transplantation*

270 Changes in bacterial community composition were profiled throughout the experiment.
271 The microbiota of control communities remained stable (**Fig. 3A**). The relative abundance of
272 *Bacilli* and *Gammaproteobacteria* increased in mice receiving the antibiotic cocktail by day 3
273 (**Fig. 3A**), though the overall bacterial load and richness remained low (**Fig. 1B,C**).
274 By day 9, co-housed mice were significantly enriched for TAC ASVs from the *Tannerellaceae*,
275 *Prevotellaceae*, and *Muribaculaceae* families, and *Lactobacillaceae* ASVs that were not
276 associated with either supplier, relative to mice without transplantation (**Fig. 3B**). Mice
277 receiving cecal or fecal transplants were also enriched for these *Lactobacillaceae* ASVs, along
278 with un-associated *Enterobacteriaceae* ASVs (**Fig. 3B**). This may reflect increased
279 aerotolerance and colonization of uninhabited gastrointestinal tract niches. *Bacteroidaceae*
280 ASVs associated with the original TAC communities were enriched in mice receiving fecal or
281 cecal transplants (**Fig. 3B**). *Enterobacteriaceae* ASVs were significantly enriched in mice
282 receiving cecal transplant compared to co-housed mice, while co-housed mice were enriched
283 for *Muribaculaceae* ASVs.

284 TAC-associated ASVs from the *Muribaculaceae* family were significantly enriched in
285 all mice receiving a microbiota transfer at day 15, regardless of method (**Fig. 3C**). TAC
286 *Bacteroidaceae* ASVs were enriched in mice receiving a cecal transplant, while TAC-
287 associated *Akkermansiaceae* ASVs were enriched in mice receiving a fecal transplant
288 compared to the 'no transfer' and co-housed groups. JAX-associated *Erysipelotrichaceae*
289 ASVs were the first to recover in antibiotic-treated mice without a transplant and were
290 significantly enriched by day 15 compared to co-housed mice or mice receiving a fecal or cecal
291 transplant (**Fig. 3C**).

292 By day 21, significant differences in bacterial taxa enrichment were observed across
293 groups (**Fig. 3D**). TAC *Staphylococcaceae* ASVs were enriched in the 'no transfer' and fecal
294 transplant groups compared to co-housed and cecal transplant recipient mice, while TAC
295 *Lactobacillaceae* ASVs were enriched in the 'no transfer' group compared to the transplant
296 groups. Notably, *Christensenellaceae* ASVs, not associated with either supplier, were

297 enriched in the ‘no transfer’ group compared to all transplantation groups. Several JAX-
298 associated taxa, including *Ruminococcaceae*, *Lachnospiraceae*, *Erysipelotrichaceae*, and
299 *Clostridiaceae*, were enriched in the ‘no transfer’ group compared to all transplant groups. The
300 fecal transplant groups exhibited distinct enrichment patterns, including higher levels of TAC-
301 associated *Staphylococcaceae* and JAX-associated *Acholeplasmataceae* compared to co-
302 housed or cecal transplant recipient mice. JAX *Acholeplasmataceae* were also enriched in the
303 ‘no transfer’ group compared to co-housed or cecal transplant recipient mice. Distinct
304 transplantation methods differentially enriched specific bacterial taxa over time, with co-
305 housing favoring *Muribaculaceae* and certain donor-associated lineages earlier, while fecal
306 and cecal transplants more strongly enriched for *Bacteroidaceae*, *Enterobacteriaceae*, and
307 *Akkermansiaceae*; mice without transplants exhibited recovery of native JAX-associated taxa
308 and unique enrichments not observed in other groups by day 21.
309

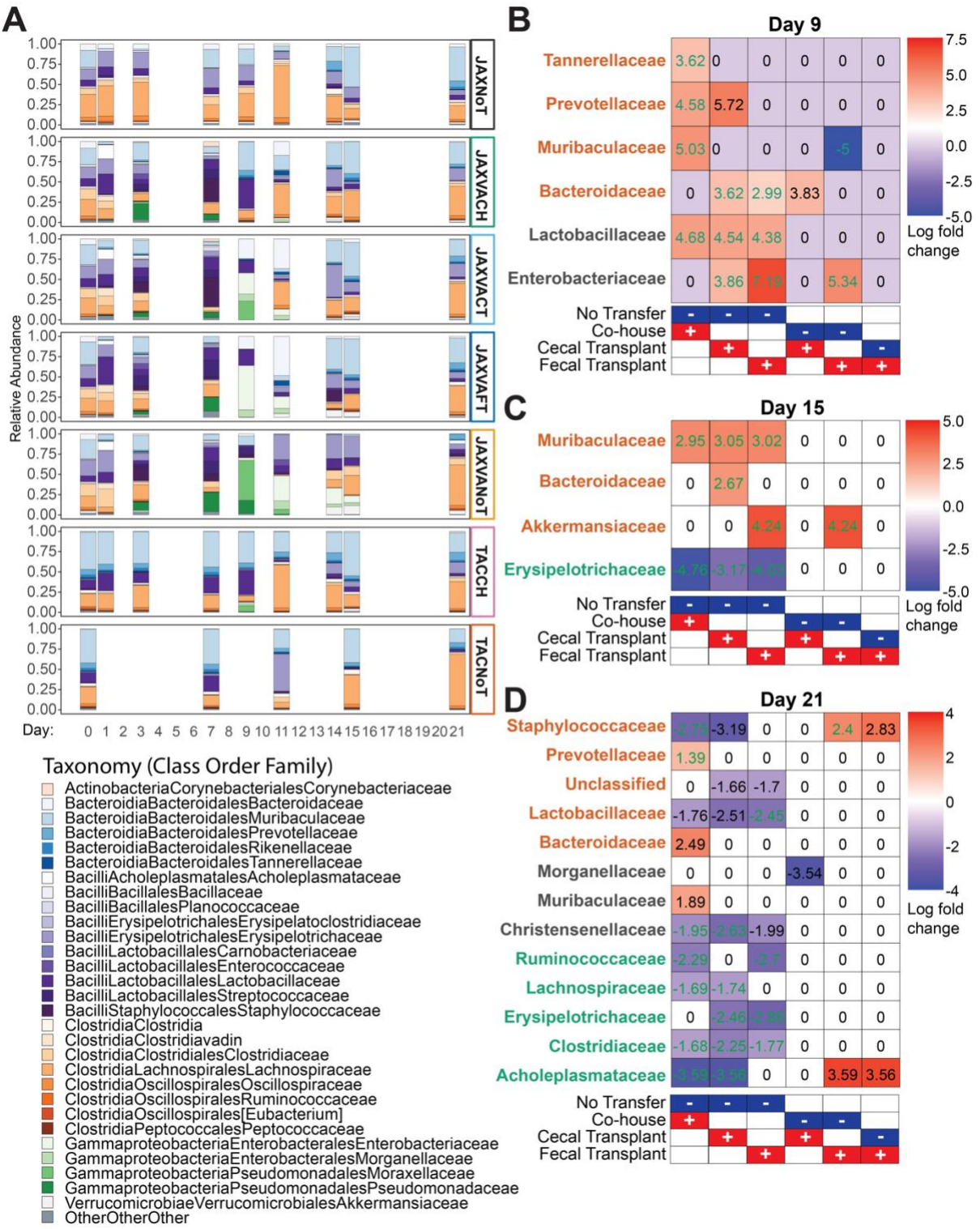

Figure 3. Specific bacterial taxa are enriched across transplantation methods. (A) Mean relative abundance of bacterial families throughout the course of the experiment in each of the treatment groups, averaged across all samples on each day. (**B-D**) Bacterial families associated with original bacterial communities of mice from Taconic (orange), Jackson (green) or neither/both (black) that were significantly enriched or depleted for the comparisons shown below each plot as determined using ANCOM-BC2. Panels show results from days 9 **(B)**, 15 **(C)**, and 21 **(D)**. Log fold change values in green remained significant after applying a stringent mixed directional FDR control.

320

321 *Bacterial diversity and community composition differ across gastrointestinal sites but not the*
322 *method of transfer*

323 Bacterial diversity and community composition varied across gastrointestinal sites and
324 treatment groups. Lower richness was consistently observed in ileal contents compared to
325 cecal contents and stool, as well as at all sites in mice without microbiota transfer after
326 antibiotic treatment (**Fig. 4A**). Stool richness trended higher in transplanted mice than JAX
327 controls but lower than TAC controls, suggesting incomplete bacterial taxa transfer. PCoA
328 illustrated community composition differences, with samples clustering according to treatment
329 and site (**Fig. 4B**). Samples from JAX mice treated with antibiotics but no transfer clustered
330 together, away from samples from transplanted mice and control communities, with samples
331 from the same gastrointestinal site clustering together. To compare community compositions
332 across treatments, PCoA was performed on samples subset by the gastrointestinal site (**Figs.**
333 **4C-E**). Ileal, cecal, and stool communities of JAX co-housed mice were closely aligned with
334 TAC mice, while ileal communities of JAX fecal or cecal transplantation mice clustered
335 separately (**Fig. 4C**), a difference that was not as pronounced in cecal or stool samples (**Figs.**
336 **4D, E**). These findings provide insights into the dynamics of bacterial community re-
337 establishment across microbiota transplantation methods.

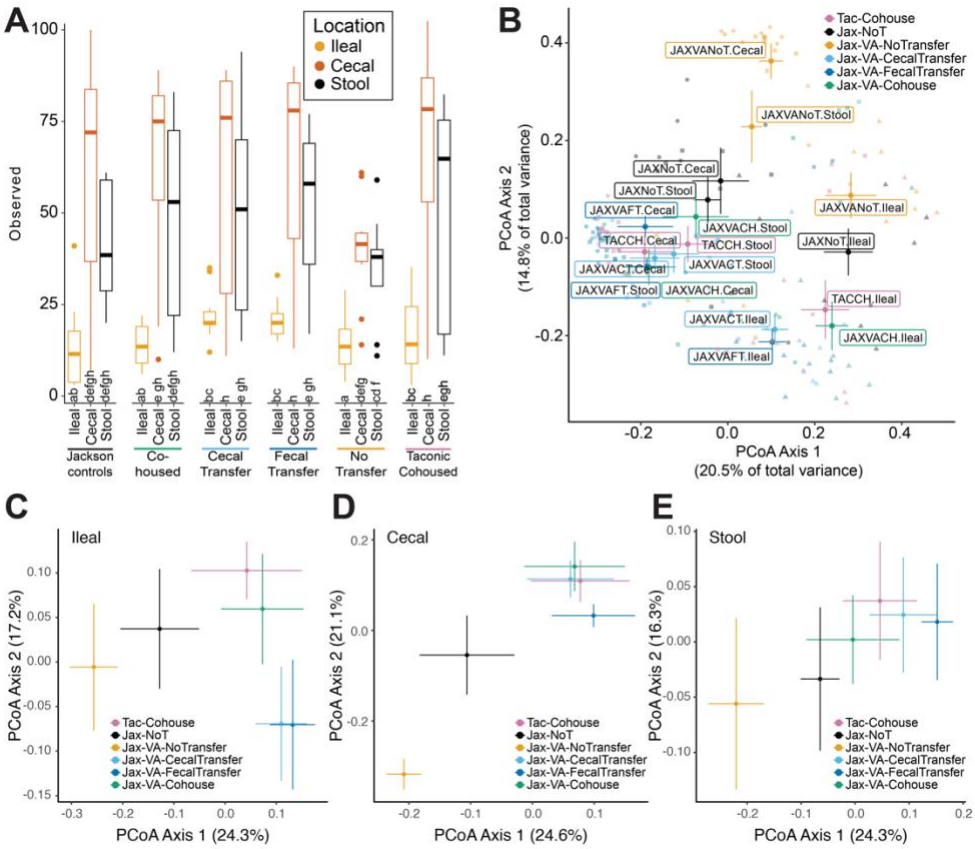

Figure 4. Bacterial diversity and community composition across different body sites and treatment groups. (**A**) Bacterial richness, the number of bacterial taxa observed in cecal, ileal, and stool samples across different groups, including Jackson controls, co-housed, cecal transfer, fecal transfer, no transfer, and Taconic controls. The letters under each bar indicate significant groupings, those with the same letter were not significantly different from one another. Observed richness was compared using a linear mixed-effects model with sequencing library as a random effect, post hoc comparison of marginal means were Tukey-adjusted; significance groups are indicated by differing letters (α = 0.05). (**B**) Plot of Principal Coordinate Analysis (PCoA) of Unweighted UniFrac Distances illustrating bacterial community composition from cecal, ileal, and stool samples, across each method of transplantation, including Jackson controls and cohoused Taconic donors. PCoA of Unweighted UniFrac Distances of samples on Day 21 across treatment groups from (**C**) ileal contents, (**D**) cecal contents, or (**E**) stool.

354 *Viral Community is Depleted Post-Antibiotics*

355 We examined the viral response to antibiotic treatment, noting a significant reduction
356 in bacterial load and diversity over the first week (**Figs. 1B, C**). Short-read shotgun sequencing
357 of DNA from viral-like particles (VLPs) assessed the impact of antibiotics on viral communities.
358 Viral richness (unique contigs from sequencing data) was compared from days 0 to 7 between
359 TAC and JAX controls and antibiotic-treated JAX mice treated. Read counts were normalized
360 to reduce library batch effects. Viral richness dropped significantly from 596 ± 84 (mean ± SE)
361 unique viral contigs on day 0 to 34 ± 2 on day 7 (**Extended Data Fig. 2A**). This pattern
362 persisted when contigs with clear viral signatures were analyzed and when aggregated into
363 clusters representing viral species, genera, and families (**Extended Data Fig. 2A**). The
364 reduction in viral richness indicates viral populations' susceptibility to bacterial community
365 disruptions, likely due to their dependence on bacterial hosts. A notable shift in viral community
366 composition, primarily driven by antibiotic treatment, was observed in PCoA of Jaccard
367 distances (**Extended Data Fig. 2B**). The separation along axis 1 was mainly between
368 antibiotic-treated and untreated groups, highlighting antibiotics' substantial impact on viral
369 community composition. Similar results were found when considering only high-quality viral
370 contigs or different taxonomic ranks (**Extended Data Fig. 2B**).

371

372 *Co-housing facilitates more rapid transfer of donor viral communities*

373 To evaluate the effects of different microbiota transfer methods on viral communities
374 in antibiotic-treated mice, we compared viral richness and community composition post-
375 transplantation. Samples were collected from days 7 to 14 to observe viral population
376 reestablishment. This analysis included all contigs from short sequencing of VLPs, avoiding
377 biases from viral annotation and prediction algorithms. Viral richness, measured by unique
378 viral contigs, did not uniformly increase across all groups after antibiotics ceased. By day 9,
379 co-housed JAX mice showed a quicker rise in viral richness than other groups, with no
380 significant difference from TAC mice (**Fig. 5A**). Viral richness was low in mice with fecal or
381 cecal transfers, or no transfer, at this point. By day 11, viral richness increased in all groups,

382 and while transplantation groups had lower richness than Taconic donors, the difference was
383 not significant. Antibiotic-treated mice without transplants had significantly lower viral richness,
384 which only slightly increased by day 11. By day 14, viral richness in all transfer groups
385 converged, similar to untreated controls, indicating successful re-colonization.

386 We assessed the impact of transplantation methods on viral community composition
387 using PCoA of Jaccard distances. Results indicated a gradual alignment of viral communities
388 in fecal and cecal transplanted mice with TAC donor profiles between days 9 and 11, achieving
389 full convergence by day 14 (**Fig. 5B**). Co-housed mice showed rapid convergence with donor
390 profiles by day 9, suggesting co-housing enhances efficient viral transfer. In contrast,
391 antibiotic-treated mice without transplants experienced delayed recovery, remaining distinct
392 from donor and control profiles until the final sampling day, gradually nearing the original JAX
393 community by day 14.

394 These findings highlight the critical role of microbiota transplantation in reestablishing
395 viral communities. Co-housing was the most effective for rapid and complete viral transfer,
396 while fecal and cecal transplants also supported successful colonization, though more slowly.
397 Mice without transplants showed delayed and incomplete viral community recovery,
398 emphasizing the need for external microbial inputs to restore gut virome diversity and
399 composition post-antibiotic treatment.

400

401 *Transfer of Taconic-associated viruses to Jackson mice*

402 To monitor virus movement between TAC and JAX mice, viral contigs were
403 categorized as TAC, JAX, or neither/both, based on their prevalence and abundance in
404 samples from the first week of the experiment (34 TAC and 50 JAX samples) without
405 antibiotics. Out of 6,249 contigs, 2,535 were TAC-associated and 1,129 were JAX-associated.
406 Antibiotic treatment significantly reduced the richness and relative abundance of JAX-
407 associated viruses (**Figs. 5C-F**). TAC and JAX control mice maintained consistent viral
408 richness and abundance (**Figs. 5C-F**), with TAC mice having more unique viral genome
409 contigs than JAX controls (**Figs. 5C, E**).

410 After microbiota transplantation, TAC-associated virus richness and abundance in co-
411 housed JAX mice was not significantly different from TAC donors by day 9 (**Figs. 5C, D**). By
412 day 9, TAC-associated virus relative abundance in fecal and cecal transplant recipients was
413 similar to donors (**Fig. 5D**), though diversity was lower (**Fig. 5C**). By day 11, four days after
414 transplantation, TAC-associated virus abundance in fecal or cecal transplant recipients
415 dropped well below donor levels (**Figs. 5D, F**). In contrast, co-housed mice maintained
416 relatively stable TAC-associated virus abundance. This decline was accompanied by a slight
417 resurgence of JAX-associated viruses on day 11 (**Figs. 5D, F**), but this rebound was not
418 sustained, except in JAX antibiotic-treated mice without transplantation, where JAX-
419 associated viruses persisted (**Figs. 5D, F**).

420 Despite only receiving two gavages of fecal or cecal contents, the number of unique
421 viral genome fragments in transplanted mice increased, with detectable TAC-associated virus
422 levels rising even after one week (**Figs. 5C, E**). However, TAC-associated virus richness in
423 JAX mice with cecal or fecal transplants remained significantly different from TAC donors one
424 week after gavage, on day 14 (**Figs. 5C, E**).

425 Viral diversity in JAX mice treated with antibiotics and no transplantation remained
426 depleted throughout the experiment (through day 14), despite JAX-associated virus
427 abundance returning to untreated JAX control and day 0 levels by day 11 (**Figs. 5C-F**). This
428 indicates a long-lasting impact of antibiotics on viral diversity in mice without microbial
429 transplants, despite partial recovery of JAX-associated viral abundance.

430 These findings underscore the complexity of viral community dynamics post-
431 microbiota transplantation, with co-housing being the most effective method for rapidly
432 restoring donor-associated viral communities. While fecal and cecal transplants also facilitated
433 donor virus colonization, the process was slower and less consistent when considering viral
434 richness and abundance.

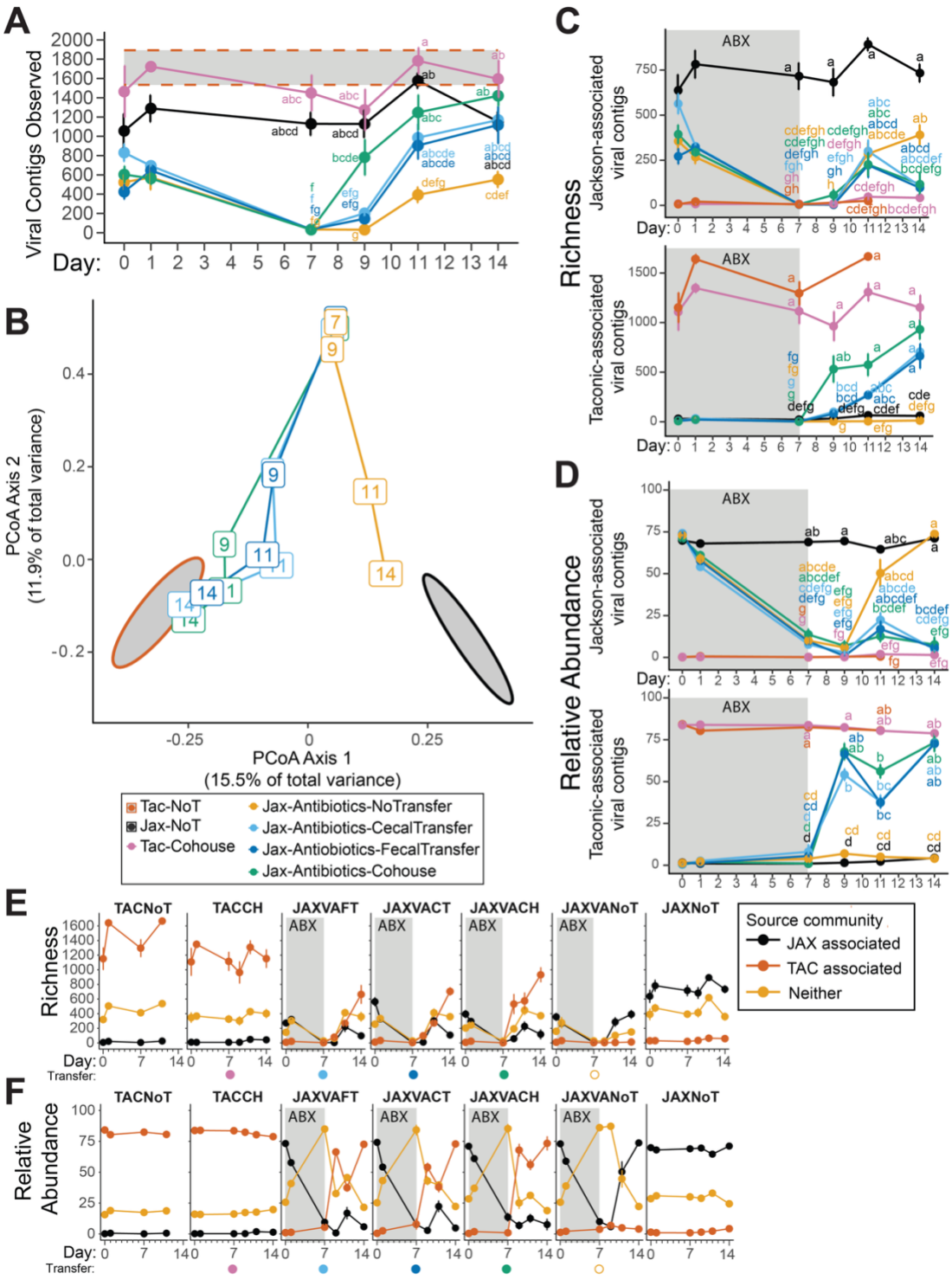

Figure 5. Cohousing of mice reconstitutes the viral microbiota more rapidly than fecal or cecal transplant. (**A**) Viral richness from days 7 through 14 of the experiment shows the rapid recovery of viral diversity following transplantation. The letters next to each point indicate significant groupings, those with the same letter were not significantly different from one another by pairwise Kruskal-Wallis followed by Bonferroni's correction for multiple comparisons with an alpha threshold of 0.05 (**B**) Principal Coordinate Analysis of Jaccard distances calculated from contig read counts across two weeks of the experiment illustrate the change in community composition following antibiotic treatment and microbiota transplantation. Ellipses (95% confidence) represent the baseline fecal viral communities of untreated Jackson (Jax-NoT) and Taconic (Tac-NoT) mice. (**C**) Richness and (**D**) relative

446 abundance of viral contigs defined as (i) Jackson or (ii) Taconic-associated throughout the
447 course of the experiment. The letters next to each point indicate significant groupings, those
448 with the same letter were not significantly different from one by pairwise Kruskal-Wallis
449 followed by Bonferroni's correction for multiple comparisons with an alpha threshold of 0.05.
450 The (**E**) richness and (**F**) relative abundance of viral contigs associated with mice from
451 Jackson, Taconic, or neither/both, over the first two weeks of the experiment. n = 6-11
452 samples per treatment group and timepoint, for all groups excluding TACNoT controls (n =
453 1-5)
454

455

456 *Binning viral genomes confirms rapid microbial transfer following cohousing*

457 Contigs were binned into homogeneous groups representing individual viral
458 genomes using CoCoNet[37], based on sequence composition and coverage variation. 1,525
459 contigs were assigned to 629 unique bins (mean 2.4 contigs per bin, 426 bins with only one
460 contig). Bins were categorized as JAX- or TAC-associated, or neither/both, according to
461 previous contig classifications. No bins contained both JAX and TAC-associated contigs,
462 allowing entire bins to be classified based on the presence of any TAC- or JAX-associated
463 contigs (**Figs. 6A-E**). The richness of JAX-associated bins significantly decreased by day 7
464 in antibiotic-treated mice (**Fig. 6B**). The richness of TAC-associated bins increased
465 significantly on day 9 in co-housed mice (**Figs. 6A, C**), but did not reach similar levels until
466 day 14 in fecal or cecal transplant mice. Additionally, the average abundance of bins was
467 quantified based on sequencing read depth, normalized by bin length and sample
468 sequencing depth. The average abundance of JAX bins (RPKM) slightly decreased after
469 antibiotic treatment and was significantly lower on day 9 in mice with microbiota
470 transplantation (**Fig. 6D**). The average abundance of TAC bins sharply increased in all
471 transplant mice on day 9 (**Fig. 6E**). These findings align with our annotation free contig-level
472 analysis, showing a rapid increase in viral richness in co-housed mice compared to those
473 with fecal or cecal transplants (**Figs. 5C, 6C**). Meanwhile, the average abundance (RPKM)
474 of Taconic bins increased in all transplant groups by day 9, mirroring the increased relative
475 abundance observed in the contig-based analysis (**Figs. 5D, 6E**).

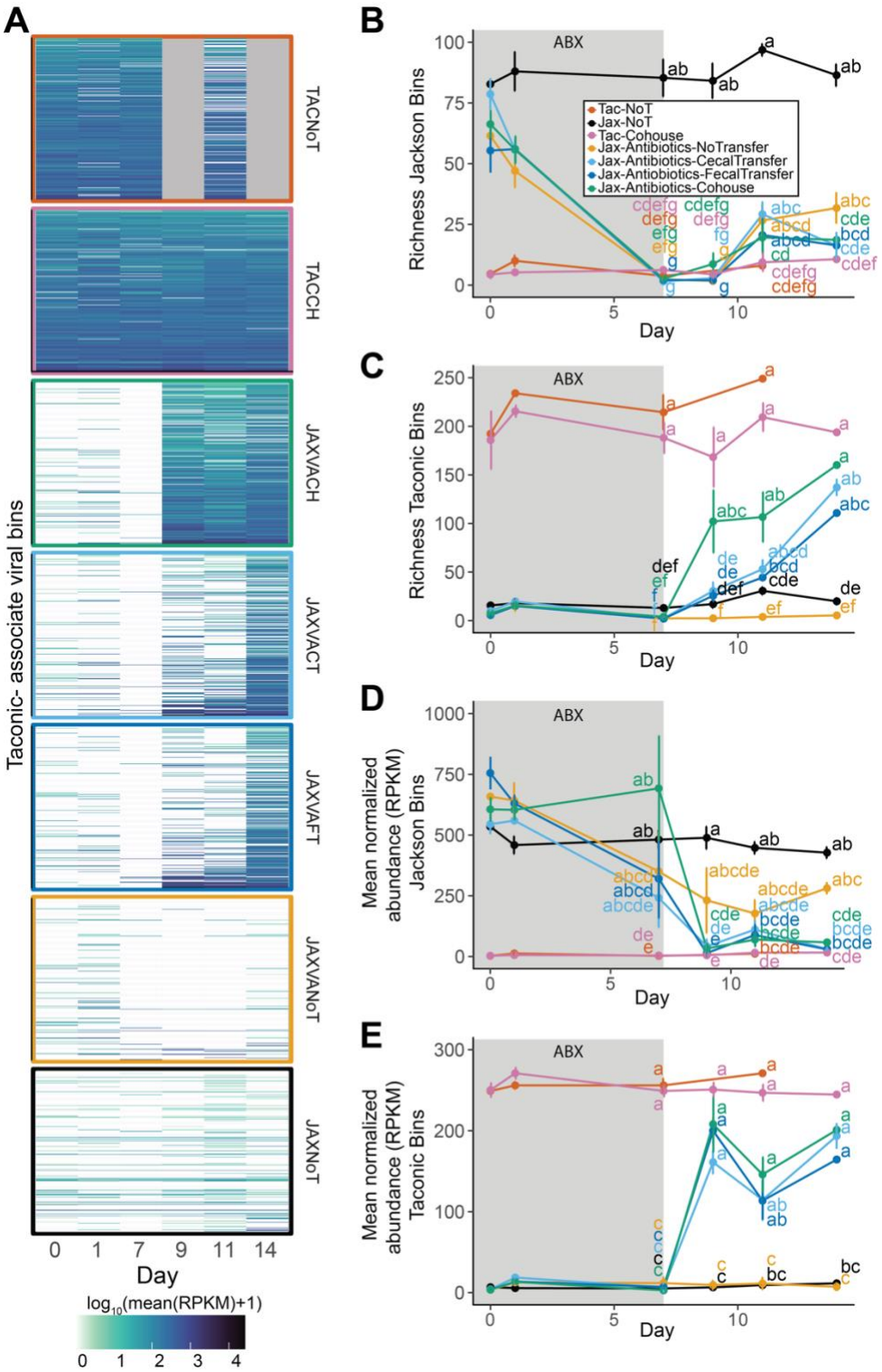

Figure 6. Binning viral genomes confirms rapid microbial transfer following cohousing (**A)** Heatmap illustrating the richness of Taconic-associated viral bins over time in each treatment and control group as indicated on the right side of each panel. Line plots of the richness of (**B**) Jackson- and (**C**) Taconic-associated viral bins and mean normalized abundance of (**D**) Jackson- and (**E**) Taconic-associated viral bins over the course of the experiment. The letters next to each point indicate significant groupings, Those with the same letter were not significantly different from one another by Kruskal-Wallis test followed by Bonferroni correction for multiple comparisons with an alpha of 0.05. n = 6-11 samples per treatment group and timepoint, for all groups excluding TACNoT controls (n = 1-5)

486

487 *Dynamics of bacteriophages predicted to target discriminatory bacterial taxa*

488 We examined the dynamics of phages targeting bacterial families with differential
489 abundance during transplantation. *Tannerellaceae*, *Prevotellaceae*, *Muribaculaceae*,
490 *Bacteroidaceae*, *Lactobacillaceae*, *Enterobacteriaceae*, *Akkermansiaceae*, and
491 *Erysipelotrichaceae* distinguished treatment groups at days 9 and 15 (**Figs. 3B, C**). Using
492 iPHoP[38], we assessed the predicted bacterial host range for filtered phage contigs. No
493 phages were predicted to target *Erysipelotrichaceae* or *Prevotellaceae*, and
494 *Akkermansiaceae*-targeting phages were rare and not significantly different across groups.
495 The abundance of phages targeting the remaining bacterial families varied over time (**Fig.**
496 **7A**). Phages targeting *Bacteroidaceae* were elevated on day 9 in cecal and fecal transplant
497 recipients, aligning with bacterial data (**Fig. 3B**). Most phages in transplant recipients were
498 temperate and not specifically linked to the original JAX or TAC communities (**Fig. 7B**), with
499 a few originally TAC-associated. JAX controls maintained JAX-associated phages targeting
500 *Bacteroidaceae*, predicted to be virulent. Also mirroring the abundance of their bacterial
501 hosts, *Enterobacteriaceae*-targeting phages peaked on day 9 in fecal transplant recipients
502 (**Figs. 7A, B**). All *Lactobacillaceae*-hosted phages were temperate and increased on day 9
503 in transplant groups (**Figs. 7A, B**). *Muribaculaceae*-hosted phages were not temperate, with
504 elevated abundance on day 9 in co-housed mice (**Figs. 7A, B**). Although many
505 *Muribaculaceae*-targeting phages were predicted to be virulent, their abundance still
506 matched their bacterial hosts (**Fig. 3B**). Despite *Tannerellaceae* bacterial enrichment on day
507 9 in co-housed mice, their targeting phages were not elevated. Phage abundance closely
508 mirrored their predicted bacterial hosts, suggesting induction of temperate phages post fecal
509 or cecal transplant, in contrast to transfer of virulent phage specifically targeting a high-
510 abundance bacterial community member, *Muribaculaceae,* in the context of co-housing.

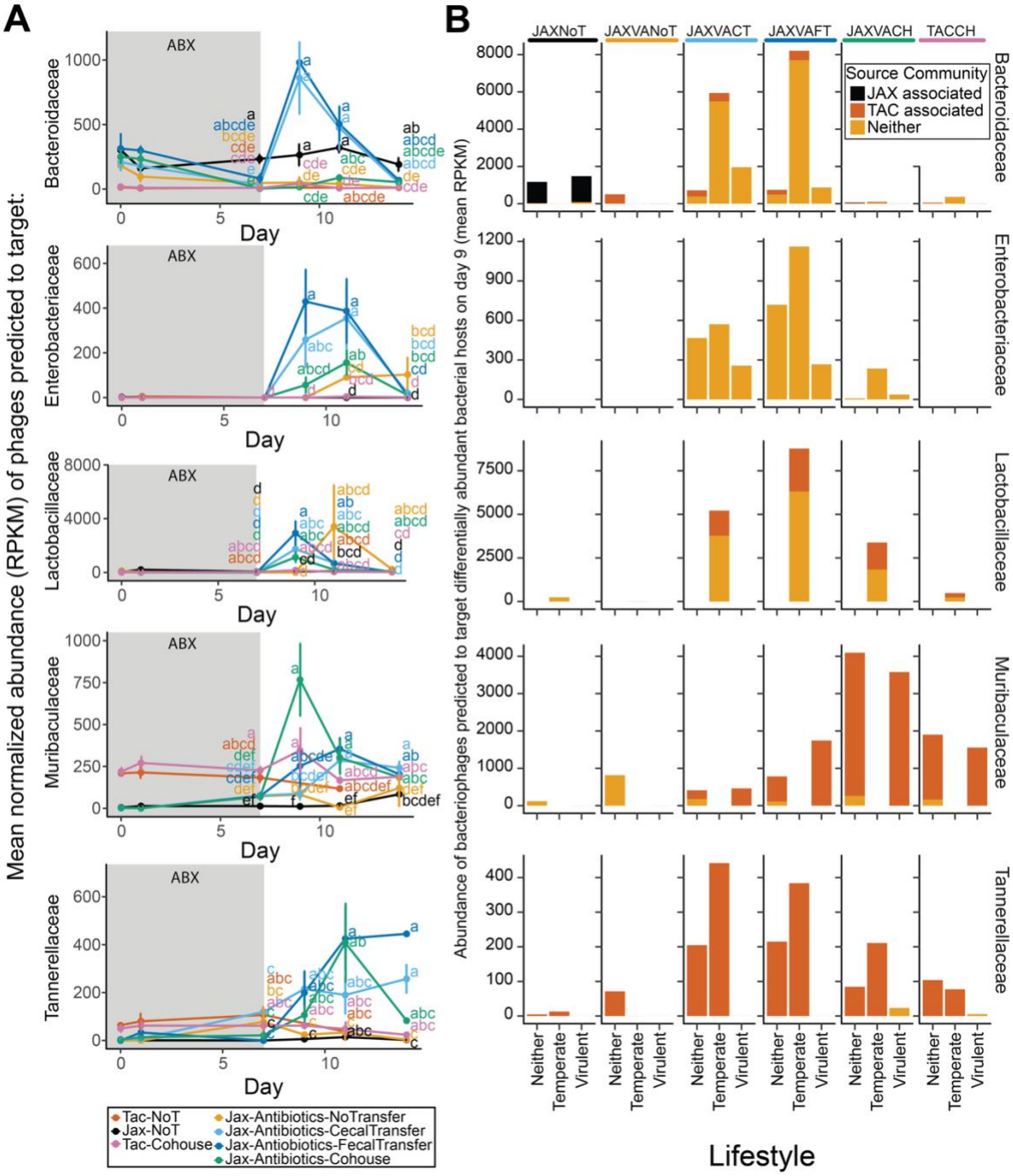

Figure 7. Abundance of bacteriophages mirrors discriminatory bacterial hosts. (**A**) The mean normalized Reads Per Kilobase per Million mapped reads (RPKM) abundance of phage bins predicted to target bacteria that were differentially abundant on day 9 (**Fig. 3B**) or day 15 (**Fig. 3C**), over time. Other bacterial families were either not predicted to be hosts for phages in this dataset, or were not significantly different between any of the groups at the timepoints test (Akkermansiaceae). The letters next to each point indicate significant groupings, those with the same letter were not significantly different from one another by Kruskal-Wallis test followed by Bonferroni correction for multiple comparisons with an alpha of 0.05. (**B**) Bar plots illustrating the abundance (mean RPKM) of phage bins targeting discriminatory bacterial taxa on day 9. Each column represents a treatment group. Within each plot, phages are split based on their predicted lifestyle. Rows are faceted by the family of the predicted bacterial host. n = 6-11 samples per treatment group and timepoint, for all groups excluding TACNoT controls (n = 1-5)

Discussion

This study compared co-housing, fecal, and cecal transplantation in antibiotic-treated mice to reconstitute bacterial and viral communities[22,23,31,39]. Transplanting donor microbiota allows researchers to examine how composition influences health and disease. However, there's a lack of systematic comparisons of commonly used transfer methods. We addressed this gap by assessing the efficiency, dynamics, and ecological outcomes of three widely used techniques. Our findings are relevant for improving experimental methods and enhancing the reproducibility of mouse-based studies on host-microbe interactions.

Our study indicates that co-housing is the most effective method for rapid microbiota transfer, quickly reconstituting both bacterial and viral communities. Sustained microbial exchange through natural behaviors like coprophagy and direct contact mirrors ecological interactions in natural settings. This efficiency aligns with previous studies showing that co-housing facilitates the transfer of donor-associated microbial taxa more robustly than gavage methods[31,40]. Co-housed mice rapidly reconstitute microbial diversity and functionality, making it useful for time-sensitive microbiota establishment. Fecal and cecal transplantation, though less efficient in the short term, achieved comparable outcomes by day 21. These methods may still be valuable in experimental scenarios where co-housing is impractical, but the slower pace of microbial establishment emphasizes the importance of considering time frames in experiments. Researchers should select transplantation methods that align with study goals to optimize reproducibility and minimize variability.

Antibiotic cocktail treatment significantly reduced intestinal bacterial loads within a day, suggesting that shorter treatment duration from the currently commonly-used 1-2 weeks before microbiota transfer would still be effective. Mice without transplantation showed delayed and incomplete microbiota recovery. This limited natural recolonization indicates insufficient native microbial recovery to restore pre-treatment diversity within two weeks, but does highlight potential for gut microbiota resiliency over the longer term.

553 The study highlighted the interdependence of bacterial and viral dynamics, reflecting
554 the ecological relationships between bacteriophages and their hosts. Antibiotics rapidly
555 depleted bacteria, leading to a slightly delayed but robust reduction in phage communities.
556 Co-housed mice quickly established donor-associated bacterial taxa like *Muribaculaceae* and
557 *Tannerellaceae*, along with their phages. In contrast, early introduction of bacteria such as
558 *Bacteroidaceae*, *Lactobacillaceae*, and *Enterobacteriaceae* via fecal or cecal transplant, was
559 linked to temperate phages targeting these hosts, which were not always main members of
560 the donor's viral community. These phages likely emerged via induction from donor pioneering
561 bacteria during early transplantation. The synchronized reconstitution seen with co-housing
562 emphasizes the role of ecological interactions in microbial recovery, suggesting that co-
563 housing may offer a more natural environment for community establishment.
564 The site-specific variation in microbial recovery across gastrointestinal regions
565 underscores the complexity of microbiota reconstitution. The distinct microbial diversity and
566 composition between ileal, cecal, and fecal samples emphasize the importance of sampling
567 multiple regions to capture microbiota dynamics. These findings align with previous work
568 showing anatomical differences in microbial communities and their functions [41–44].
569 Systematic evaluations of transplantation methods across different contexts are
570 crucial. Future studies should investigate how donor-recipient compatibility, microbial
571 complexity, and host genotype influence outcomes. While this study focused on bacterial and
572 viral communities, incorporating fungi and archaea will provide a more comprehensive
573 understanding. Advancements in functional and longitudinal metagenomic analyses, coupled
574 with improved animal models, will enhance our ability to study microbiota establishment and
575 its implications for host health and disease. As we expand comparisons to new donor/recipient
576 sources and microbial compartments, our comprehensive virome profiling pipeline, utilizing
577 contig-based, classification-agnostic, and robust binning and classification methods, will
578 ensure consistent capture of even poorly characterized or emerging viral populations across
579 different experimental models. While characterization of human viral communities has broadly
580 lagged behind the study of bacterial communities, the virome of experimental mice remains

581 even more enigmatic. Our method successfully facilitated virome analysis and comparisons,
582 and it could also be extended to analyze other poorly annotated microbes like fungi and
583 archaea.

584 This study systematically compared microbiota transplantation methods, refining
585 experimental approaches in microbiome research and revealing ecological and functional
586 dynamics underlying microbial reconstitution. These insights will facilitate tailoring of
587 transplantation methods to individual studies, thereby enhancing reproducibility and
588 translational potential, and advancing our understanding of the microbiome's role in health
589 and disease.

590

591 **Materials and Methods**

592 **Mice and Treatments**

593 WT C57BL/6J (stock no. 000664) mice were purchased from Jackson Laboratories (JAX) and
594 C57BL/6N (stock #B6), murine pathogen free health standard, mice were purchased from
595 Taconic Biosciences (TAC) and maintained at Washington University School of Medicine
596 under specific-pathogen-free conditions according to University guidelines. Female mice,
597 aged six to eight weeks, were exclusively used in all experiments to facilitate cohousing
598 experiments. Experimental mice were co-housed with up to two mice of the same sex per
599 cage with autoclaved standard chow pellets and water provided *ad libitum*. Cages of female
600 mice were treated at 6 weeks of age with an antibiotic cocktail VNA [1 g/L ampicillin, 1 g/L
601 neomycin, 0.5 g/L vancomycin (Sigma, St. Louis, MO)] in drinking water for 7 days.

602 For fecal and cecal transplants, donor mice were euthanized by CO_2 asphyxiation, and
603 dissections were performed under sterile conditions in a biosafety cabinet using Clidox- and
604 ethanol-sterilized tools. Fecal pellets or cecal contents were collected into sterile 50 mL
605 conical tubes and homogenized in phosphate-buffered saline (PBS). Resulting homogenates
606 were administered to recipient mice by oral gavage using sterile syringes and 20-gauge
607 curved gavage needles on day 8 and day 9, with each mouse receiving approximately 200–
608 400 µL. For co-housing, Jackson recipient mice were paired with Taconic donor mice on Day
609 7. Co-housed pairs were maintained in fresh cages with autoclaved bedding, food, and water.
610 Each experimental replicate included control groups: untreated JAX and TAC mice and
611 antibiotic-treated JAX mice with no subsequent transplantation, beyond the antibiotic-treated
612 groups undergoing fecal transplant, cecal transplant, or co-housing. Fecal samples were
613 collected longitudinally, and all mice were monitored daily for behavior, health status, and cage
614 conditions. Special care was taken to prevent cage flooding and ensure adequate chow and
615 water access, particularly during antibiotic treatment. After transplantation or co-housing, all
616 mice received autoclaved drinking water without antibiotics for the remainder of the
617 experiment. All animal procedures were approved by and conducted in compliance with
618 Washington University's Institutional Animal Care and Use Committee (IACUC) guidelines.

619 The experiment was repeated for a total of three independent experiments, with data
620 combined in subsequent analyses.
621
622 **16S rRNA gene Illumina sequencing**
623 Phenol:chloroform-extracted DNA from fecal pellets was used for both 16S rRNA gene
624 qPCR and sequencing. SYBR green qPCR for the 16S rRNA gene was performed with 515F
625 (5'-GTGCCAGCMGCCGCGGTAA-3') and 805R (5'-GACTACCAGGGTATCTAATCC-3')
626 primers to detect the V4 hypervariable region. Samples were prepared in three batches with
627 samples from across experiments and treatment groups semi-randomized, in a supervised
628 manner, between the pools.
629 Primer selection and PCRs were performed as described previously [14]. Briefly, each
630 sample was amplified in triplicate with Golay-barcoded primers specific for the V4 region
631 (F515/R806), combined, and confirmed by gel electrophoresis. PCR reactions contained
632 18.8μL RNase/DNase-free water, 2.5μL 10X High Fidelity PCR Buffer (Invitrogen), 0.5μL 10
633 mM dNTPs, 1μL 50 mM MgSO4, 0.5μL each of the forward and reverse primers (10 μM final
634 concentration), 0.1μL Platinum High Fidelity Taq (Invitrogen) and 1.0μL genomic DNA.
635 Reactions were held at 94°C for 2 min to denature the DNA, with amplification proceeding for
636 26 cycles at 94°C for 15s, 50°C for 30s, and 68°C for 30s; a final extension of 2 min at 68°C
637 was added to ensure complete amplification. Amplicons were pooled and purified with 0.6x
638 Agencourt Ampure XP beads (Beckman-Coulter) according to the manufacturer's instructions.
639 The final pooled samples, along with aliquots of the three sequencing primers, were sent to
640 the Center for Genome Sciences (Washington University School of Medicine) for sequencing
641 by the 2x250bp protocol with the Illumina MiSeq platform.
642 The resulting FASTQ files were processed using the DADA2 pipeline (v1.28.0)
643 implemented in Nephele (version 2024_Jan_16, commit: 71b6a72)[32]. Initial quality
644 assessment was conducted to determine appropriate truncation and filtering parameters.
645 Reads were trimmed to remove low-quality bases and sequencing primers and truncated
646 based on quality scores to ensure high-confidence base calls[45,46]. Specifically, reads were

647 truncated at the position where the quality score dropped below a threshold (default: 4)[47,48].
648 Reads with expected errors exceeding a set threshold (default: 5) were discarded to further
649 enhance data quality. Forward and reverse reads were merged, requiring a minimum overlap
650 of 12bp and allowing for zero mismatches in the overlapping region to ensure accurate
651 reconstruction of the target amplicon[49,50]. Chimeric sequences were identified and removed
652 using the consensus method to prevent false-positive operational taxonomic units (OTUs).
653 Taxonomic classification was performed using the Ribosomal Database Project (RDP)
654 classifier, with a minimum bootstrap confidence threshold of 40 for taxonomic assignments
655 and the SILVA v138.1 database[51]. Additionally, a phylogenetic tree was constructed using
656 MAFFT for multiple sequence alignment and FastTree2 for tree building, facilitating
657 downstream phylogenetic analyses[52,53]. The output included an amplicon sequence variant
658 (ASV) table, taxonomic assignments, and phylogenetic relationships, providing a
659 comprehensive dataset for subsequent diversity and composition analyses. All analyses were
660 conducted using default parameters unless otherwise specified, adhering to best practices for
661 16S rRNA gene sequence processing to ensure accurate and reproducible results. One
662 sample ("TACNoT.MTP2.D11.74") was excluded due to lack of stool at the time of DNA
663 extraction. Twelve ASVs assigned to Eukaryota, Mitochondria, or Chloroplast were removed,
664 and one sample that no longer contained bacterial reads were excluded from downstream
665 analysis.
666
667 **Bacterial ecological and distance analyses**
668 Bacterial community composition and ecological metrics were assessed using both
669 alpha and beta diversity analyses. Alpha diversity metrics, including observed richness and
670 Shannon diversity, were calculated to evaluate within-sample diversity. Beta diversity was
671 assessed using unweighted and weighted UniFrac distances to capture phylogenetic
672 differences between samples. These analyses were implemented using the 'phyloseq' and
673 'vegan' R packages, which offer comprehensive tools for ecological and diversity analyses.
674 Principal coordinate analysis (PCoA) was performed to visualize patterns in beta diversity

675 across treatment groups and time points[54,55]. Pairwise comparisons between groups were
676 conducted using PERMANOVA with Bonferroni corrections to identify statistically significant
677 differences (alpha = 0.05). These analyses provided insights into the ecological shifts in
678 bacterial communities associated with different transplantation methods and recovery stages.
679 All figures were generated in R using ggplot2[56].
680
681 **Identifying bacterial taxa associated with each vendor**
682 Bacterial taxa specific to each vendor were identified using ASVs derived from 16S
683 rRNA gene sequencing. Taxa were classified as Jackson-associated or Taconic-associated
684 based on their differential prevalence and abundance in fecal samples collected from
685 untreated mice during the first week of the experiment (days 0-7). Samples were limited to
686 those without antibiotic treatment to accurately capture baseline community differences.
687 Differential abundance analyses were conducted using the DESeq2 pipeline, with ASVs
688 assigned taxonomy using the SILVA database. Significant differences were determined using
689 an adjusted p-value threshold of 0.01 and a combined log2(fold change) cutoff of ±4.
690 Prevalence was calculated as the proportion of samples in which a given ASV was detected
691 within each vendor group. To incorporate abundance and prevalence, a combined fold-change
692 metric was calculated by summing the log2(fold change) from differential abundance analysis
693 and the log2(prevalence ratio) between the two groups. Statistical and prevalence-based
694 analyses were compared to confirm associations, and taxa that did not meet these criteria
695 were categorized as non-supplier-specific.
696
697 **Predicting functional capacity of bacterial communities**
698 Functional capacities of bacterial communities were inferred from 16S rRNA gene
699 sequencing data using the PICRUSt2 (v. 2.5.3) pipeline. ASVs were mapped to predicted
700 genes and metabolic pathways using the MetaCyc database. Differentially abundant pathways
701 were identified using DESeq2 with an alpha threshold of 0.05. Comparisons were made
702 between antibiotic-treated recipient mice (co-housed, fecal transplantation, or cecal

703 transplantation groups) and control communities from untreated Jackson and Taconic mice.
704 Functional convergence over time was assessed across treatment groups to evaluate the
705 recovery of microbial metabolic potential.
706
707 **Taxonomic changes following transplantation**
708 Changes in bacterial taxonomic composition were assessed longitudinally using 16S
709 rRNA gene sequencing. ASVs were classified into taxonomic families, and relative
710 abundances were tracked over time in recipient mice across different transplantation methods
711 (co-housing, fecal, and cecal). Differentially enriched taxa were identified using ANCOM-BC2
712 (v. 2.6.0), and significant changes were determined using Kruskal-Wallis tests with Bonferroni
713 corrections for multiple comparisons (alpha = 0.05). Taxonomic dynamics were visualized
714 using stacked bar plots and principal coordinate analyses (PCoA) of unweighted UniFrac
715 distances.
716 **Statistical comparisons across gastrointestinal sites**
717 To evaluate differences in observed species richness across experimental groups, we
718 fit a linear mixed-effects model using the lmer function from the lme4 package (v. 1.1-35.5),
719 with Sample Type (gastrointestinal site) and Condition (transplantation method) specified as
720 fixed effects and Sequencing Library included as a random effect to account for variation
721 across sequencing batches[57]. ANOVA as implemented in the lmerTest package (3.1-3) was
722 used to test the significance of fixed effects[58]. Post hoc comparisons of estimated marginal
723 means were conducted using the lsmeans function withing the emmeanspackage (v. 1.10.3)
724 with Tukey's HSD correction for multiple testing[59]. Group-level differences were visualized
725 using compact letter display from the multcompView package (v. 0.1-10), where groups not
726 sharing a letter are significantly different at $\alpha = 0.05$[60].
727 **Virome Illumina sequencing and analysis**
728 Viral communities were characterized using short-read Illumina sequencing of viral-
729 like particles (VLPs) extracted from fecal samples. DNA was purified from VLPs, and libraries
730 were prepared using standard protocols. Sequencing was performed on an Illumina platform,

731 generating paired-end reads. Reads were assembled into contigs using Flye, which is
732 optimized for accurate assembly of viral genomes from metagenomic data. Viral contigs were
733 identified using stringent criteria for viral hallmark genes and annotated taxonomically using
734 Cenote-Taker2, a tool designed for comprehensive identification and annotation of eukaryotic
735 and prokaryotic viruses.

736 To account for batch effects associated with preparation of viral sequencing pools, raw
737 viral count tables were first converted to a DESeq2[36] dataset using the phyloseq_to_deseq2[55]
738 function with a design formula including VP, Source, Day, Antibiotics, and PostFMT. Counts
739 were log-transformed using variance-stabilizing transformation (VST) with blind = FALSE.
740 Batch effects attributable to viral preparation were then removed using the removeBatchEffect
741 function from the limma package, specifying the model design to preserve variation due to
742 biological covariates[61]. The resulting batch-corrected abundances were rounded to the
743 nearest integer, and any negative values were set to zero before being re-integrated into the
744 phyloseq object for downstream analysis. Samples where fewer than ten unique viral contigs
745 were detected were filtered out of subsequent analyses.

746

747 **Viral ecological and distance analyses**

748 Viral community composition and ecological dynamics were assessed using alpha
749 diversity metrics (e.g., richness) and beta diversity measures (e.g., Jaccard distances). These
750 analyses were implemented using the 'phyloseq' and 'vegan' R packages, which provide
751 robust tools for microbial ecological analyses. Principal coordinate analysis (PCoA) was
752 conducted to visualize temporal changes in viral community structure across treatment
753 groups. Pairwise comparisons between groups were performed using PERMANOVA with
754 Bonferroni corrections for multiple comparisons (alpha = 0.05). Viral communities were further
755 classified as Jackson-associated, Taconic-associated, or non-supplier-specific based on their
756 prevalence and abundance in control communities. Ecological metrics were integrated with
757 bacterial data to explore host-virus interactions during microbiota transplantation. Source

758 discriminatory viral contigs were defined using the combined fold-change metric described for
759 bacteria above.

760 **Hierarchical clustering of viral contigs**

761 We employed a hierarchical clustering approach to categorize viral contigs into
762 taxonomic units based on amino acid identity (AAI) and average nucleotide identity (ANI).
763 Initial protein-coding genes were predicted from input contigs using Prodigal[62] (v2.6.3; in
764 metagenomic mode. All-versus-all BLASTP alignments (BLAST+[63], v2.7.1) were performed to
765 compute AAI values, filtered to retain pairs with ≥20% AAI, ≥10% shared genes, and ≥8
766 homologous proteins. These filtered edges underwent Markov Clustering (MCL[64] v22.282)
767 with an inflation parameter of 1.2 to define family-level clusters. Each family cluster was
768 recursively processed using stricter thresholds (≥40% AAI, ≥20% shared genes, ≥16
769 homologs; MCL inflation=2.0) to resolve genus-level clusters. Finally, genus clusters were
770 subjected to nucleotide-level ANI analysis via BLASTn and checkV's anicalc.py (checkV[65]
771 v1.0.1), with vOTUs (viral operational taxonomic units) delineated at ≥95% ANI and ≥85%
772 coverage.

773 **Viral classification and binning**

774 To further identify viral contigs, we then applied a two-tier filtering approach to these
775 binned contigs. First, any contig shorter than 1,500 bp was excluded. Contigs were then
776 assessed with VirSorter2 (retaining those with a viral score ≥50) and DeepVirFinder (retaining
777 those with a score ≥0.7 and p-value ≤0.05)[66,67]. Contigs that did not meet these primary criteria
778 were retained if they contained more viral genes than host genes and harbored at least one
779 viral hallmark gene as identified by Cenote Taker2[68]. This pipeline yielded 2,262 putative viral
780 contigs. Taxonomic assignments of these viral contigs were determined using vContact3,
781 while iPHoP and PHATyp were employed for host and lifestyle (temperate vs. virulent)
782 predictions, respectively[38,69]. CheckV was used to assess genome quality and
783 completeness[65]. Contigs were binned using CoCoNet, which discards sequences shorter than
784 2,048 base pairs by deafult[37].

Bins were classified based on the aggregated predictions of the contigs they contained. Bins were labeled by their inferred source community if they contained any contigs from one of the sources—Taconic-associated or Jackson-associated—and labeled "Neither/Both" otherwise. No bins contained both Taconic-associated and Jackson-associated contigs. Next, lifestyle predictions (virulent vs. temperate) were consolidated at the bin level by checking whether any contigs in a bin were classified as temperate or virulent, and no contigs within the bin were predicted to be of the other lifestyle. No lifestyle classification was assigned to bins with a mixture of predictions at the contig level. Of the classified bins, 165 were predicted to be temperate while 138 were predicted to be virulent. Finally, host family assignments were integrated by examining the taxonomic predictions for each contig within a bin: bins containing contigs from a single family were assigned that family, bins spanning multiple families in a single phylum were labeled with the phylum followed by "_spp," and bins spanning multiple phyla were labeled "multi."

Use of Large Language Models

Large language models, including Google's Gemini, OpenAI' ChatGPT, and Apple Intelligence Writing Tools were used in the preparation of this manuscript. These tools were used to edit text and included the use of the following prompts: "Make concise," "Make concise while preserving figure callouts." All text output from these models was subsequently edited and confirmed for scientific accuracy by an author.

Acknowledgments: We acknowledge all members of the Baldridge laboratory for helpful discussions as well as member of June Round's laboratory.

Funding: This work was supported by the National Institutes of Health (NIH) grants R01AI139314, R01AI173360, and U01AT012998 (M.T.B.), and the Crohn's and Colitis Foundation Litwin IBD Pioneers Award #1065897 (M.T.B.). E.A.K. was supported by NSF grant DGE-1745038/DGE-2139839 and NIH grant F31AI167499. H.M. was supported by NIH R25 GM103757. J.S.W. was supported by NIH T32AI007172. The funders did not play any role in the study design, data collection and analysis, decision to publish, or preparation of the manuscript.

Author contributions: J.S.W performed data analysis generated figures and wrote the manuscript. M.E.S., H.M., S.A., M.H., E.A.K., L.A.S. and L.F. performed the experiments. M.E.S., H.M., S.A., and M.T.B. designed the project. L.A.C.C. and A.R contributed analysis of viral data. M.T.B. contributed to the writing of the manuscript. All authors read and edited the manuscript.

Inclusion and Ethics: We affirm that this work was conducted in accordance with recognized ethical standards in research and reporting. Contributions were made in line with Nature Portfolio authorship guidelines, and all co-authors have approved this version of the manuscript. We are committed to inclusive and equitable collaboration, and we have actively worked to ensure fair representation and acknowledgment of contributions from all team members, regardless of career stage, identity, or background. Where applicable, trainees involved in the study received formal instruction in responsible conduct of research.

Competing interests: We declare no competing interests.

Data and materials availability: The data from this study are tabulated in the main paper and supplementary materials. All reagents are available from M.T.B. under a material transfer agreement with Washington University. Additionally, all sequencing data generated in this study, including 16S rRNA gene amplicon data and virome shotgun metagenomic data, have been deposited in the European Nucleotide Archive (ENA), under accession number PRJEB55403 and publicly accesible upon acceptance. Data files, metadata, and scripts used for analysis are available at Zenodo (**10.5281/zenodo.15191166)** and will be made publicly accessible upon publication. Mapping between raw files submitted to ENA all relevant metadata are available at Zenodo (**10.5281/zenodo.15191166).**

Code availability statement: Scripts and code used for analysis are available on Zenodo (**10.5281/zenodo.15191166)** and will be made publicly accessible upon publication.

841 **References**

842 1. Sommer, F. & Bäckhed, F. The gut microbiota — masters of host development and
843 physiology. *Nat. Rev. Microbiol.* **11**, 227–238 (2013).
844 2. Round, J. L. & Mazmanian, S. K. The gut microbiota shapes intestinal immune responses
845 during health and disease. *Nat. Rev. Immunol.* **9**, 313–323 (2009).
846 3. Oliphant, K. & Allen-Vercoe, E. Macronutrient metabolism by the human gut
847 microbiome: major fermentation by-products and their impact on host health.
848 *Microbiome* **7**, 91 (2019).
849 4. Li, T.-T. *et al.* Microbiota metabolism of intestinal amino acids impacts host nutrient
850 homeostasis and physiology. *Cell Host Microbe* **32**, 661-675.e10 (2024).
851 5. Donald, K. & Finlay, B. B. Early-life interactions between the microbiota and immune
852 system: impact on immune system development and atopic disease. *Nat. Rev. Immunol.*
853 **23**, 735–748 (2023).
854 6. Lambring, C. B. *et al.* Impact of the Microbiome on the Immune System. *Crit. Rev.*
855 *Immunol.* **39**, 313–328 (2019).
856 7. Graham, D. B. & Xavier, R. J. Conditioning of the immune system by the microbiome.
857 *Trends Immunol.* **44**, 499–511 (2023).
858 8. Villarino, N. F. *et al.* Composition of the gut microbiota modulates the severity of
859 malaria. *Proc. Natl. Acad. Sci. U. S. A.* **113**, 2235–2240 (2016).
860 9. Baldridge, M. T. *et al.* Commensal microbes and interferon-λ determine persistence of
861 enteric murine norovirus infection. *Science* **347**, 266–269 (2015).
862 10. Winkler, E. S. *et al.* The Intestinal Microbiome Restricts Alphavirus Infection and
863 Dissemination through a Bile Acid-Type I IFN Signaling Axis. *Cell* **182**, 901-918.e18
864 (2020).

865 11. Turnbaugh, P. J. *et al.* An obesity-associated gut microbiome with increased capacity for
866 energy harvest. *Nature* **444**, 1027–1031 (2006).
867 12. Ridaura, V. K. *et al.* Gut microbiota from twins discordant for obesity modulate
868 metabolism in mice. *Science* **341**, 1241214 (2013).
869 13. Gehrig, J. L. *et al.* Effects of microbiota-directed foods in gnotobiotic animals and
870 undernourished children. *Science* **365**, eaau4732 (2019).
871 14. Di Luccia, B. *et al.* Combined Prebiotic and Microbial Intervention Improves Oral Cholera
872 Vaccination Responses in a Mouse Model of Childhood Undernutrition. *Cell Host*
873 *Microbe* **27**, 899-908.e5 (2020).
874 15. Britton, G. J. *et al.* Defined microbiota transplant restores Th17/RORγt+ regulatory T cell
875 balance in mice colonized with inflammatory bowel disease microbiotas. *Proc. Natl.*
876 *Acad. Sci. U. S. A.* **117**, 21536–21545 (2020).
877 16. Britton, G. J. *et al.* Microbiotas from Humans with Inflammatory Bowel Disease Alter the
878 Balance of Gut Th17 and RORγt+ Regulatory T Cells and Exacerbate Colitis in Mice.
879 *Immunity* **50**, 212-224.e4 (2019).
880 17. Kennedy, E. A., King, K. Y. & Baldridge, M. T. Mouse Microbiota Models: Comparing
881 Germ-Free Mice and Antibiotics Treatment as Tools for Modifying Gut Bacteria. *Front.*
882 *Physiol.* **9**, (2018).
883 18. Witjes, V. M., Boleij, A. & Halffman, W. Reducing versus Embracing Variation as
884 Strategies for Reproducibility: The Microbiome of Laboratory Mice. *Animals* **10**, 2415
885 (2020).
886 19. Schloss, P. D. Identifying and Overcoming Threats to Reproducibility, Replicability,
887 Robustness, and Generalizability in Microbiome Research. *mBio* **9**, 10.1128/mbio.00525-
888 18 (2018).

889 20. Huttenhower, C., Finn, R. D. & McHardy, A. C. Challenges and opportunities in sharing
890 microbiome data and analyses. *Nat. Microbiol.* **8**, 1960–1970 (2023).
891 21. Moossavi, S., Fehr, K., Khafipour, E. & Azad, M. B. Repeatability and reproducibility
892 assessment in a large-scale population-based microbiota study: case study on human
893 milk microbiota. *Microbiome* **9**, 41 (2021).
894 22. Zhang, C. *et al.* Transfer efficiency and impact on disease phenotype of differing
895 methods of gut microbiota transfer. *Sci. Rep.* **12**, 19621 (2022).
896 23. Ericsson, A. C. & Franklin, C. L. Manipulating the Gut Microbiota: Methods and
897 Challenges. *ILAR J.* **56**, 205–217 (2015).
898 24. Borin, J. M. *et al.* Fecal virome transplantation is sufficient to alter fecal microbiota and
899 drive lean and obese body phenotypes in mice. *Gut Microbes* **15**, 2236750 (2023).
900 25. Rasmussen, T. S. *et al.* Faecal virome transplantation decreases symptoms of type 2
901 diabetes and obesity in a murine model. *Gut* **69**, 2122–2130 (2020).
902 26. Federici, S. *et al.* Targeted suppression of human IBD-associated gut microbiota
903 commensals by phage consortia for treatment of intestinal inflammation. *Cell* **185**,
904 2879-2898.e24 (2022).
905 27. Gogokhia, L. *et al.* Expansion of Bacteriophages Is Linked to Aggravated Intestinal
906 Inflammation and Colitis. *Cell Host Microbe* **25**, 285-299.e8 (2019).
907 28. Hsu, B. B. *et al.* Dynamic Modulation of the Gut Microbiota and Metabolome by
908 Bacteriophages in a Mouse Model. *Cell Host Microbe* **25**, 803-814.e5 (2019).
909 29. Pfeiffer, J. K. & Virgin, H. W. Transkingdom control of viral infection and immunity in the
910 mammalian intestine. *Science* **351**, aad5872 (2016).
911 30. Brunse, A. *et al.* Fecal filtrate transplantation protects against necrotizing enterocolitis.
912 *ISME J.* **16**, 686–694 (2022).

913 31. Caruso, R., Ono, M., Bunker, M. E., Núñez, G. & Inohara, N. Dynamic and Asymmetric
914 Changes of the Microbial Communities after Cohousing in Laboratory Mice. *Cell Rep.* **27**,
915 3401-3412.e3 (2019).
916 32. Weber, N. *et al.* Nephele: a cloud platform for simplified, standardized and reproducible
917 microbiome data analysis. *Bioinforma. Oxf. Engl.* **34**, 1411–1413 (2018).
918 33. Callahan, B. J. *et al.* DADA2: High-resolution sample inference from Illumina amplicon
919 data. *Nat. Methods* **13**, 581–583 (2016).
920 34. Douglas, G. M. *et al.* PICRUSt2 for prediction of metagenome functions. *Nat. Biotechnol.*
921 **38**, 685–688 (2020).
922 35. Caspi, R. *et al.* The MetaCyc database of metabolic pathways and enzymes and the
923 BioCyc collection of pathway/genome databases. *Nucleic Acids Res.* **44**, D471-480
924 (2016).
925 36. Love, M. I., Huber, W. & Anders, S. Moderated estimation of fold change and dispersion
926 for RNA-seq data with DESeq2. *Genome Biol.* **15**, 550 (2014).
927 37. Arisdakessian, C. G., Nigro, O. D., Steward, G. F., Poisson, G. & Belcaid, M. CoCoNet: an
928 efficient deep learning tool for viral metagenome binning. *Bioinformatics* **37**, 2803–2810
929 (2021).
930 38. Roux, S. *et al.* iPHoP: An integrated machine learning framework to maximize host
931 prediction for metagenome-derived viruses of archaea and bacteria. *PLOS Biol.* **21**,
932 e3002083 (2023).
933 39. Robertson, S. J. *et al.* Comparison of Co-housing and Littermate Methods for Microbiota
934 Standardization in Mouse Models. *Cell Rep.* **27**, 1910-1919.e2 (2019).

935 40. Lundberg, R. *et al.* Human microbiota-transplanted C57BL/6 mice and offspring display
936 reduced establishment of key bacteria and reduced immune stimulation compared to
937 mouse microbiota-transplantation. *Sci. Rep.* **10**, 7805 (2020).
938 41. Hollister, E. B., Gao, C. & Versalovic, J. Compositional and Functional Features of the
939 Gastrointestinal Microbiome and Their Effects on Human Health. *Gastroenterology* **146**,
940 1449–1458 (2014).
941 42. Mu, C., Yang, Y., Su, Y., Zoetendal, E. G. & Zhu, W. Differences in Microbiota
942 Membership along the Gastrointestinal Tract of Piglets and Their Differential Alterations
943 Following an Early-Life Antibiotic Intervention. *Front. Microbiol.* **8**, 797 (2017).
944 43. Shkoporov, A. N. *et al.* Viral biogeography of the mammalian gut and parenchymal
945 organs. *Nat. Microbiol.* **7**, 1301–1311 (2022).
946 44. Anders, J. L. *et al.* Comparing the gut microbiome along the gastrointestinal tract of
947 three sympatric species of wild rodents. *Sci. Rep.* **11**, 19929 (2021).
948 45. Andrews, S. Babraham Bioinformatics - FastQC A Quality Control tool for High
949 Throughput Sequence Data.
950 https://www.bioinformatics.babraham.ac.uk/projects/fastqc/.
951 46. Ewels, P., Magnusson, M., Lundin, S. & Käller, M. MultiQC: summarize analysis results
952 for multiple tools and samples in a single report. *Bioinforma. Oxf. Engl.* **32**, 3047–3048
953 (2016).
954 47. Martin, M. Cutadapt removes adapter sequences from high-throughput sequencing
955 reads. *EMBnet.journal* **17**, 10–12 (2011).
956 48. Bolger, A. M., Lohse, M. & Usadel, B. Trimmomatic: a flexible trimmer for Illumina
957 sequence data. *Bioinformatics* **30**, 2114–2120 (2014).

958 49. Magoč, T. & Salzberg, S. L. FLASH: fast length adjustment of short reads to improve
959 genome assemblies. *Bioinformatics* **27**, 2957–2963 (2011).
960 50. Streett, D. dstreett/FLASH2. (2025).
961 51. Quast, C. *et al.* The SILVA ribosomal RNA gene database project: improved data
962 processing and web-based tools. *Nucleic Acids Res.* **41**, D590–D596 (2013).
963 52. Katoh, K. & Standley, D. M. MAFFT Multiple Sequence Alignment Software Version 7:
964 Improvements in Performance and Usability. *Mol. Biol. Evol.* **30**, 772–780 (2013).
965 53. Price, M. N., Dehal, P. S. & Arkin, A. P. FastTree 2 – Approximately Maximum-Likelihood
966 Trees for Large Alignments. *PLoS ONE* **5**, e9490 (2010).
967 54. Oksanen, J. *et al.* vegan: Community Ecology Package. 2.6-8
968 https://doi.org/10.32614/CRAN.package.vegan (2001).
969 55. McMurdie, P. J. & Holmes, S. phyloseq: An R Package for Reproducible Interactive
970 Analysis and Graphics of Microbiome Census Data. *PLOS ONE* **8**, e61217 (2013).
971 56. Wickham, H. *et al.* ggplot2: Create Elegant Data Visualisations Using the Grammar of
972 Graphics. (2024).
973 57. Bates, D., Mächler, M., Bolker, B. & Walker, S. Fitting Linear Mixed-Effects Models Using
974 lme4. *J. Stat. Softw.* **67**, 1–48 (2015).
975 58. Kuznetsova, A., Brockhoff, P. B. & Christensen, R. H. B. lmerTest Package: Tests in Linear
976 Mixed Effects Models. *J. Stat. Softw.* **82**, 1–26 (2017).
977 59. Lenth, R. V. *et al.* emmeans: Estimated Marginal Means, aka Least-Squares Means.
978 (2025).
979 60. Graves, S., Piepho, H.-P. & Selzer, L. multcompView: Visualizations of Paired
980 Comparisons. (2024).

981 61. Ritchie, M. E. *et al.* limma powers differential expression analyses for RNA-sequencing
982 and microarray studies. *Nucleic Acids Res.* **43**, e47 (2015).
983 62. Hyatt, D. *et al.* Prodigal: prokaryotic gene recognition and translation initiation site
984 identification. *BMC Bioinformatics* **11**, 119 (2010).
985 63. Camacho, C. *et al.* BLAST+: architecture and applications. *BMC Bioinformatics* **10**, 421
986 (2009).
987 64. Van Dongen, S. Graph Clustering Via a Discrete Uncoupling Process. *SIAM J. Matrix Anal.*
988 *Appl.* **30**, 121–141 (2008).
989 65. Nayfach, S. *et al.* CheckV assesses the quality and completeness of metagenome-
990 assembled viral genomes. *Nat. Biotechnol.* **39**, 578–585 (2021).
991 66. Guo, J. *et al.* VirSorter2: a multi-classifier, expert-guided approach to detect diverse DNA
992 and RNA viruses. *Microbiome* **9**, 37 (2021).
993 67. Ren, J. *et al.* Identifying viruses from metagenomic data using deep learning. *Quant.*
994 *Biol.* **8**, 64–77 (2020).
995 68. Tisza, M. J., Belford, A. K., Domínguez-Huerta, G., Bolduc, B. & Buck, C. B. Cenote-Taker 2
996 democratizes virus discovery and sequence annotation. *Virus Evol.* **7**, veaa100 (2021).
997 69. Shang, J., Tang, X. & Sun, Y. PhaTYP: predicting the lifestyle for bacteriophages using
998 BERT. *Brief. Bioinform.* **24**, bbac487 (2023).
999